# Electrolytic Co-Deposition Mechanisms, Texture Layers, and Residual Stresses in Nanocomposite Coatings Processes: A Review

## Noureddine Elboughdiri[1,2*]

[1]Chemical Engineering Department, College of Engineering, University of Ha'il, Ha'il, Saudi Arabia
[2]Chemical Engineering Process Department, National School of Engineers Gabes, University of Gabes, Gabes, Tunisia
Email: *ghilaninouri@yahoo.fr

## Abstract

The composite coating has gained wider attention due to its property to protect materials used in energy, bridges, offshore platforms, underground pipelines, and the aviation industry from corrosion and deterioration. In this work, a literature review was conducted about the processes of nanocomposite coating, the mechanisms of electrolytic co-deposition, the texture of layers, and the residual stresses. An important aspect, residual stress, was emphasized, which represents the persistent stress after removing the external force affecting a metal in the plastic region. Because it cannot be measured directly and may be determined by measuring strain and indirect methods, the sources and methods for measuring residual stresses (XRD, SEM, TEM, EDS) were described in the last section to provide a comprehensive overview. Based on the thorough analysis of the published literature, it was concluded that nanoparticles could be electrodeposited with Ni on an Al substrate using a direct current and Ni sulfamate as an electrolytic solution, and Nickel will not reside on the oxide layer covering Al, so chemical changes are needed to prepare the Al surface. In addition, texture changes with the thickness of the coated layer must be investigated.

## 1. Introduction

The material's surface is the first to encounter harsh external conditions, and its

deterioration can end up in the catastrophic failure of the bulk material. Therefore, the material used in the automotive and aviation industry must be protected by applying a coating to minimize surface deterioration, prevent wear, protect from corrosion, and improve mechanical properties. Thin sheets of aluminum alloys have been used extensively in the commercial aircraft industry for the past 50 years thanks to their availability, chemical stability, and physical properties like low density. Aluminum has a density of 2.77 g/cm$^3$, juxtaposed to steel (7.86 g/cm$^3$). Hence, aluminum is lighter and has a higher strength-to-weight ratio than steel, even if it has lower wear resistance. Aluminum 2024-T3 alloy contains 4% - 5% Cu [1] [2] [3] [4]. Corrosion of this alloy can be accelerated due to a galvanic pair created between Al and Cu. The T3 indicates that the alloy solution was treated, cold-worked, and naturally aged. Therefore, it is essential to protect the alloy from harsh conditions by coating it to decrease its corrosion and wear resistance since they significantly impact economics and aircraft operations. Nickel coating protects the aluminum surface for non-chemical operating conditions. It has good adhesion properties to the coated surface and can plate uniformly over all surfaces in contact with the plating solution. The coating is preferred as a protection process for metal surfaces because it is easy to use at relatively low temperatures. As a result of the coating process, crystal-preferred orientation and residual stresses are developed on the formed layer, and both physical properties will affect the wear resistance of the coated material [5] [6] [7] [8].

In this work, we conducted a literature review of the processes of nanocomposite coating, the mechanisms of electrolytic co-deposition, the texture of layers, and the residual stresses.

## 2. Nickel Coating Processes on Aluminum

The Nickel coating process on the aluminum substrate has been shown to improve its wear resistance by applying an inexpensive, highly adhesive thin layer of another material (*i.e.*, Nickel) on the aluminum surface. Typically, aluminum plating is chosen due to its stable chemical nature, high wear resistance, availability, and shiny finish look. The coating process has two main phases: pre-coating and the actual coating.

The aluminum substrate goes through a series of chemical treatment processes that aim to change its surface's nature and enable adhesion of the coated Nickel on the substrate, as Nickel will not reside on oxides. The four substages of pre-coating are alkaline degreaser, alkaline etching, acidic etching, and zincating [1].

Following the pre-coating process, the substrate is moved to a Nickel-coating bath. Nickel plating is the deposition of a Nickel layer onto a substrate, either with an electrical current (electroplating) or without current (electroless plating). The electroplating process involves the dissolution of the anode, which is Nickel in this case, and the deposition of that metal onto the aluminum metal surface through an aqueous solution of the metal salt Nickel sulfamate. The solution provides the needed conductivity to transfer ions from the anode to the cathode.

Then, the coating reactions are done in that solution, and a direct current (DC) is applied through the anode and cathode. Theoretically, the coating process can continue until the anode is completely consumed, which is analogous to electrocoagulation, where metal ions produced from a sacrificial anode perpetuate the coagulation process [9].

The adhesion of the Nickel layer and thickness are two essential properties to take care of, as their contribution is vital in determining the coated layer's quality. In addition, the porosity and thickness distribution through the surface is also necessary.

The weight of coated Nickel and thickness of the coated layer can be calculated using Equations (1) and (2), respectively:

$$Ni_{wt} = 1.095 \times I \times t \tag{1}$$

$$\text{Thickness} = Ni_{wt} / \left( A_{coated} \times \rho_{Ni} \right) \tag{2}$$

where: $Ni_{wt}$: weight of coated Nickel (g), $I$: electric current (A), $t$: time of coating (s), $\rho_{Ni}$: density of the coated Nickel (g/cm$^3$), and $A_{coated}$: cross-sectional area of the coated layer (cm$^2$).

The critical factors that control the quality of the coating are current density (CD), duration of coating, pH of the coating bath, and mixing rate [8] [9] [10].

## 3. Nanocomposite Coating

Nanoparticles are ceramic or metallic materials in powder form with a size of around 50 nm, and they have unique chemical, mechanical, electrical, and optical properties. They are used for many applications, such as coating materials to modify their surface properties, and are added to the coating bath at the time of coating. Therefore, these particles should have known specifications like specific surface area, volume, purity, and all physicochemical specifications that can affect the coated layer [11] [12] [13].

Many methods are used to prepare nanoparticles. Some methodology involves breaking down the materials from bulk material to lower scale, while in other processes, the nanoparticles are used directly. This process requires laser abrasion, plasma synthesis, mechanical alloying or high-energy milling, sol-gel synthesis, and chemical vapor deposition. Finally, the nanoparticles are prepared through physical vapor synthesis and discrete particle encapsulation.

According to multiple published articles, most of the nanoparticles added to the coating bath are incorporated with the deposited metal matrix on the surface of the substrate. As a result, different properties of the deposited layer become noticeable because of the added nanoparticles' physicochemical and mechanical properties [12] [13] [14].

## 4. Mechanisms of Electrolytic Co-Deposition

Insoluble nanoparticles are co-deposited with the metal on the substrate surface. Two suggested models (the Gugliemi model [15] and the mathematical model

(MTM) for the electrolytic codeposition [16]) explain the electrolytic co-deposition of a particle with a metallic matrix. In the Gugliemi model, the adsorbed charge is crucial in deciding the co-deposition practicability. This model consists of two steps during which the effects of adsorption and electrophoretic attraction are responsible for the particulate incorporation in the deposited material. During the first step, a particle is adsorbed on the cathode. There is no actual contact between the particle and the cathode, as the cathode is surrounded by a layer of ions and solvent molecules. The last step occurs if the cathode's electrical field can reveal the particle's electric double layer. This model explains the CD effect on the noticed volume portion of the embedded particles. The MTM model was developed due to the need for more details. The primary assumption is that the particle will be embedded because a particular portion of the fixed ions on the particle's surface is decreased. In this model, the co-deposition may be explained as a five-step process (as shown in Table 1 and Figure 1).

Figure 1 shows the pathways of particle codeposition into a metal deposit [18]. The areas comprise the generation of ionic clouds around the particles (bulk

Table 1. Five-step process of the mathematical model (MTM) for explaining co-deposition [17] [18].

| Step | Description |
| --- | --- |
| *Step #1* | Adsorption of ionic species onto the particle surface. |
| *Step #2* | Displacement of the particle by forced convection towards the cathode's hydrodynamic boundary layer ($\delta_0$). Also, $\delta_0$ is the distance between an object and the fluid where the velocity is relatively constant. |
| *Step #3* | Diffusion of the particle through the double diffusion layer ($\delta$). |
| *Step #4* | Adsorption of the particle, still with its ionic cloud, at the cathode surface. |
| *Step #5* | Reduction of some adsorbed ionic species by which the particle becomes irreversibly incorporated in the metal matrix. |
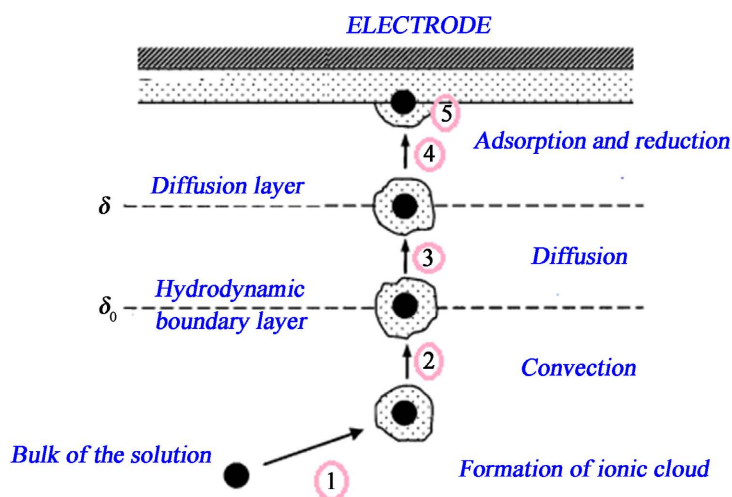


Figure 1. A schematic describing the co-deposition process of particles in a five steps reaction.

electrolyte, typical length in cm); convective movement toward the cathode (convection layer, typical length b1 mm); diffusion through a concentration boundary layer (diffusion layer, typical dimensions of hundreds of μm); electrical double layer (typical sizes of nm) followed by adsorption and entrapment of particles.

The MTM model is valid when steady-state conditions are assumed, so no change in concentration, pressure, temperature, or over-voltage occurs during the process. In addition, the surface of the cathode must be reachable for the plating solution and the associated particles. Finally, a homogeneous suspension of particles in the plating solution is maintained [16] [18].

Besides, SiC nanoparticles do not co-deposit with Nickel directly. Therefore, an additive (e.g., $Na_3Co(NO_2)_6$) is needed with Nickel to enhance the co-deposition of nano SiC co-deposition in Nickel. $Na_3Co(NO_2)_6$ is an electrolytic material that will be dissolved in water giving an anion $[Co(NO_2)_6]^{3-}$ and a cation $(Na^+)$ according to Eq. (3):

$$Na_3Co(NO_2)_6 \rightarrow 3Na^+ + \left[Co(NO_2)_6\right]^{3-} \tag{3}$$
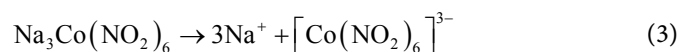
The additive reduces the distances between SiC particles. Such a decrease is due to the lower surface potential of SiC particles, which makes Van der Waals's attractive force the dominant force between molecules. Reducing the distance between SiC particles happens when the anion $[Co(NO_2)_6]^{3-}$ is adsorbed on the $Ni^+$ ions inside the coating bath. This phenomenon will neutralize the charge on the particle [13] [18].

## 5. Texture of Coatings

The crystals may line up along a preferred orientation in polycrystalline materials, forming a unique texture. This aggregation can be due to an external force resulting from mechanical or manufacturing processes on the material, such as rolling or drawing. It may also come from an atomic flux during film deposition or heat flow during solidification. Due to external forces, the crystalline lattice will change its orientation by slipping or twining in the crystal towards a stable direction. Further treatments on the oriented crystalline metal may change its texture or orient the initially random metal.

The crystallographic texture is not related to the grain size or shape. Instead, it describes a preferential alignment of the crystalline lattice of the different grains. Texture may affect the physicochemical and mechanical characteristics of the material. As an illustration, anisotropy has been noticed in tensile strength for some materials [8] [9] [10].

Many techniques have been developed to measure the texture, including hardware and computer software attached to different machines. One of the ways to express the data collected about a surface is to express them using pole figures. A pole figure can be defined as a stereographic projection with a particular orientation corresponding to the specimen that depicts the change of pole density with pole orientation for a chosen group of crystal planes [19] [20] [21] [22]. Arbitra-

rily oriented crystals will confer a pole figure with a uniform pole density; however, crystallites with a preferred orientation will make the pole density non-uniform and illustrate their projections in clusters. It is essential to know the texture of a material, as mentioned earlier, since it may affect the physicochemical properties of the material. Two types of textures may result from mechanical force applications on the fabric: *fiber texture* and *sheet texture*. In the fiber texture, the individual crystals are oriented so that a specific crystallographic orientation is parallel to an external direction. The material has rotational symmetry around an axis: in such a manner, all crystals distributed about this axis are equally probable. In the sheet texture, for rolled products, the grain lattices are often aligned concerning two external directions simultaneously (e.g., to both rolling plane normal and rolling direction). The grain orientation is fixed to axes in the sheet; a combination of transmission and reflection geometry can make a pole figure for a sheet texture. Transmission is only possible with thin samples; the reflection can be used for much thicker pieces and can cover a much larger area of the pole figure.

The existence of preferred orientation in electroplated metals and its dependence on the bath composition was proven for the first time in 1924 by Glocker *et al.* [23]. Cho *et al.* [24] studied the effect of the substrate on the texture of the electrodeposited material by coating different substrates under different conditions [25] [26]. They showed that the orientation of the co-deposited materials might depend on the texture of the substrate and the bath condition. They also reported that texture depends on the substrate for thin coatings, as the thickness of the layer increases the surface that will rely on coating conditions.

Pogrebnjak *et al.* [27] explained what Cho *et al.* [24] found by following the effect of coating conditions like CD, coating solution's composition, pH of the solution, temperature, and voltage on preferred orientation development with coatings thickness. He specified that in electrodeposition, the texture is a function of the crystal structure of the coated material and coatings besides coating conditions. The texture will depend only on coating conditions when the lattice parameter differs by more than 15% between the coated material and the coatings. If the two lattice parameters are close, then the initial layers of the coating grow independently of the coating conditions. As the coating thickness increases, the texture will depend only on the coating conditions.

Alfantazi *et al.* [28] reported that changing from steel to copper substrate does not significantly influence the coating preferred orientation. Banerjee studied the effect of coating conditions on texture. Those conditions were: bath composition, CD, pH, and the presence of impurities or ions in the coating bath. Pangarov and Vitkova [29] [30] studied the electrodeposition conditions and the developed texture. He related the texture to the electroplating coating conditions. He reported that if the coatings were deposited at high temperatures and low CD, the developed texture in metals would be (111); but, when the coatings are done at low temperatures and high CD, the generated texture in the face-centered cubic unit cell will be (110). Many cases exist when other textures are developed, like

(100), (112), (113), and (210).

Evans [31] found that the texture of electroplated Nickel is (110) when the coatings are done with higher values of internal stresses and hardness and a texture of (100) when the coatings have lower values. Those internal stresses were developed due to the electroplating process. They could be related to the binding momentum between the deposited atoms and the generated shear forces during the coating build-up.

Vadim *et al*. [32] noticed that even if the texture in the first deposited layer is random, a texture of growth with a preferred orientation will be developed. For example, the texture of plated Nickel in a sulfamate bath was firm (100) with an observed (110) texture; those coatings were deposited at a temperature of 280˚C for five hours.

El-Sherik *et al*. [33] found that a texture of (100) was developed as the CD increased in the Watt coating bath. He reported that Nickel coating of 70 μm thickness deposited from a sulfamate bath has a texture of (110) for coatings done at a temperature of 50˚C. A coating was done at a temperature lower than 40˚C, with a texture of (100). Cao stated that orientation densities of (110) and (100) depend on the cathode's CD and coating thickness, which increases with the increasing time of coatings.

Czerwinski [34] deposited Nickel from Watt's and chloride electrolytes at a temperature of 60 K, a CD of 1 and 10 A/dm$^2$, and pH values of 0.5 - 5. He obtained a (110) texture from a chloride bath and CD below 2 A/dm$^2$. The texture of (211) was obtained when a CD of 10 A/dm$^2$ was used in the chloride bath. The texture of (100) was obtained over a wide range of CDs when Nickel was deposited from Watt's solution. He mentioned that the (111) is not preferential for Nickel and cannot readily be reached in the as-deposited state of Nickel. The texture of electrodeposited Nickel depends on coating conditions like electrolyte composition, temperature, pH, CD, stirring, and organic additions. However, no theory predicts the total collection of texture findings. Various textures can be obtained for electrodeposited Nickel by controlling coatings conditions. As an example, (111) texture can be obtained for Nickel via annealing a (100) initial texture [34] [35].

## 6. Residual Stresses

Residual stress is the persistent stress after removing the external force affecting a metal in the plastic region. It cannot be measured directly. Instead, it may be determined by measuring strain and indirect methods using the elastic constants of materials to calculate the stress. Residual stresses result from the unrestored deformation in crystals due to mechanical loads. Nonetheless, in a coating process, there is no mechanical load applied. In this case, the stresses resulted from the coating nature of the chemical media in which the coating was taking place. Such media will affect how particles and grains are stacked on the surface of the coated sample [36] [37] [38].

## 6.1. Sources of Residual Stresses

Lingois *et al.* [36] examined residual stresses in dental composites. He related the generation of residual stresses to the rapid vitrification of the composite, causing considerable residual stresses that may cause the material to fail. Xianbing *et al.* [37] measured residual stresses in nanostructured coatings applied by the thermal spray technique. They reported that the thermal spraying process develops residual stresses that may result in the spallation and cracking of the coatings.

Buchmann *et al.* [38] affirmed that residual stresses could cause coatings to fail due to delamination effects in the coatings and the interface. He also confirmed that cracks would appear on the surface of the coating if the stress level reaches the ultimate strength of the coatings or leads to plastic strain in the interface. In addition, Xianbing found that grinding the sample's surface can alter the strength of residual stresses and wear resistance [37].

Jian *et al.* [39] calculated residual stresses in various coatings on a substrate. They concluded that the stresses in a plane of the film are related not only to the grain orientations but also to the direction in the plane of the film, except in (100) and (111) oriented grains. Park *et al.* studied the effect of bath parameters on the developed residual stresses for electrodeposited Nickel-phosphorus alloys. They found that the pH has the most substantial impact on residual stress formation, unlike the bath temperature and CD, which have only a slight impact. Increasing the pH reduced the tensile stresses of pure electrodeposited Nickel. Basrour *et al.* found that residual stresses depend on the electroplating conditions, mainly CD, electrolyte composition of the substrate, and the thickness of the coated layer for coatings deposited from a Nickel sulfamate bath at pH = 4 and temperature of 55˚C. They confirmed that there is no effect of CD or thermal contribution and found that residual stresses decreased as the coated layer's thickness increased [40] [41].

## 6.2. Methods for Measurement of the Residual Stress

The methods used to measure residual stress can be divided into two main categories: destructive methods, in which the sample or specimen tested is destroyed and will not be used again, like the hole drilling method, and non-destructive methods, in which no physical or chemical changes occur to the sample. The most used techniques are briefly mentioned below [39] [40] [41] [42]:

- *X-ray diffraction (XRD) method*

    The X-ray diffraction (XRD) method measures residual stresses in metals and alloys, and the spacing between lattice planes is used as a strain gauge. Before stress measurement using XRD, the sample's surface must be clean and smooth. Any scale or dirt should be removed in a process that produces no residual stress or changes the stress state of the materials, so caution is needed in choosing this process. Most scholars suggest grinding and machining, but these processes produce high stresses to a depth of 0.127 mm. In the case of coating, grinding will remove the coated layer, so the sample should be clean. Another way of separa-

tion is acid etching. Researchers affirmed that etching might produce some stress. However, different scientists confirmed that the etching influence might be neglected even if deep etching has a rough surface. The only reliable method of removing materials without introducing stress is electrolytic polishing. The specimen is suggested as an anode in the electrolytic cell. The surface must not be touched before measuring the stress, and any roughness in the surface should be avoided since the high point in the surface has a different stress value than the bulk material. If it is needed to measure the surface residual stress or the effect of some material processing, the surface should not be treated; otherwise, the results will be meaningless.

- *Scanning electron microscope* (*SEM*)

Using the scanning electron microscope (SEM), we can obtain a magnified image utilizing a beam of electrons [43]. Samples used in the SEM should be prepared to withstand the vacuum inside the chamber, so no loose powders are allowed. The samples should be conductive and must be cleaned using an ultrasonic cleaner. After the sample is prepared, it is placed in the chamber, tightly closed. Then, all the air is pumped out from the chamber and the column; an electron gun, a tungsten filament placed at the top of the column, emits a beam of electrons at high energy. The emission of the electrons and their energy are controlled by the applied voltage and the supplied electric power to the filament. The electron beam moves down the column across a chain of magnets arranged to center the electrons at a highly valid point. Scanning coils are used near the column bottom to pass the electron beam on the sample back and forth, row by row. As the beam hits any spot on the sample, another electron from the sample surface will knock out. A detector connected to the chamber enumerates such electrons and transmits the signals to an amplifier. An ultimate three-dimension image is created from the electrons sent from each point of the sample.

- *Transmission electron microscope (TEM)*

In the transmission electron microscope (TEM), a beam of monochromatic electrons is emitted from an electron gun at the column top. Those electrons are transmitted through the sample. That beam is focused to a small spot through condenser lenses, and an aperture is used to eliminate any high-angle electron. As the electrons pass through, they are influenced by both the structures and objects on the sample. Such influences are only noticed for some portions of the electronic beam sent across fractions of the sample. The transmitted beam is projected onto the viewing phosphor screen, forming an enlarged sample image.

The darker areas of the image represent those areas of the sample that fewer electrons were transmitted through, and the lighter areas of the image designate those areas of the sample that more electrons were sent through.

- *Energy dispersive x-ray spectroscopy (EDS)*

Energy dispersive X-ray spectroscopy (EDS) is a chemical microanalysis technique used with SEM and TEM. This method uses the X-ray transmitted from the sample throughout the bombardment using the electron beam to determine the elemental composition of the examined spot. When the sample is bombarded

by the SEM (or TEM) electron beam, electrons are ejected from the atoms at the sample's surface. An electron from a higher shell fills the generated electron vacancy, and an X-ray is sent to equilibrate the energy gap between the two electrons. The EDS X-ray detector determines the number of emitted x-rays and their energy. The energy of the X-ray is the feature of the element from which the X-ray was transmitted. A spectrum of the energy as a function of relative counts of the detected X-rays is acquired and examined to determine the elements in the sampled spot qualitatively and quantitatively.

## 7. Conclusion and Recommendations

Based on the collected data and interpretations through this literature review, the following conclusions and recommendations can be made:

- Nanoparticles can be electrodeposited with Nickel on an aluminum substrate using a direct current (DC) and Nickel sulfamate as the electrolytic solution.
- Nickel will not reside on the oxide layer covering aluminum, so chemical changes are necessary to prepare the aluminum surface for the coating.
- A case worth further study is the texture changes with the thickness of the coated layer. For example, a different texture was noticed for thinner coatings for the same plating conditions.

The necessity to apply new technology, such as electron energy loss spectroscopy, to study the interface between the coating and the substrate and develop a theory explaining the nature of the chemical and physical bonding between them.

## Conflicts of Interest

The author declares no conflicts of interest regarding the publication of this paper.

## References

[1] Mei, H.J., *et al.* (2022) The Additions of V and Cu on the Microstructure and Mechanical Properties of Mo-N Coatings. *Coating*, **1129**, 1-15.
https://doi.org/10.3390/coatings12081129

[2] González-Castillo, E.I., Costantini, T., Shaffer, M.S.P. and Boccaccini, A.R. (2020) Nanocomposite Coatings Obtained by Electrophoretic Co-Deposition of Poly(etheretherketone)/Graphene Oxide Suspensions. *Journal of Materials Science*, **55**, 8881-8899.
https://doi.org/10.1007/s10853-020-04632-4

[3] Maido, M., Lauri, A., Jekaterina, K., Hugo, M., Aivar, T. and Väino, S. (2021) Effective Corrosion Protection of Aluminum Alloy AA2024-T3 with Novel Thin Nanostructured Oxide Coating. *Surface and Coatings Technology*, **411**, Article ID: 126993.
https://doi.org/10.1016/j.surfcoat.2021.126993

[4] Francy, C.G.R., Julieta, T.G. and Juan, M.H.L. (2022) Differences between the Untreated and Treated Diffusion Zone in the Alclad 2024-T3 Aluminum Alloy and Hard Anodic Films. *Surface and Coatings Technology*, **429**, Article ID: 127939.
https://doi.org/10.1016/j.surfcoat.2021.127939

[5] Hirpara, J.G., Chawla, V. and Chandra, R. (2020) Investigation of Tantalum Oxynitride for Hard and Anti-Corrosive Coating Application in Diluted Hydrochloric Ac-

id Solutions. *Materials Today Communications*, **23**, Article ID: 101113. https://doi.org/10.1016/j.mtcomm.2020.101113

[6] Pinate, S., Ghassemali, E. and Zanella, C. (2022) Strengthening Mechanisms and Wear Behavior of Electrodeposited Ni-SiC Nanocomposite Coatings. *Journal of Materials Science*, **57**, 16632-16648. https://doi.org/10.1007/s10853-022-07655-1

[7] Herrera-Jimenez, E.J., Bousser, E., Schmitt, T., Klemberg-Sapieha, J.E. and Martinu, L. (2021) Effect of Plasma Interface Treatment on the Microstructure, Residual Stress Profile, and Mechanical Properties of PVD TiN Coatings on Ti-6Al-4V Substrates. *Surface and Coatings Technology*, **413**, Article ID: 127058. https://doi.org/10.1016/j.surfcoat.2021.127058

[8] Saxena, V., Uma Rani, R. and Sharma, A.K. (2006) Studies on Ultra High Solar Absorber Black Electroless Nickel Coatings on Aluminum Alloys for Space Application. *Surface and Coatings Technology*, **201**, 855-862. https://doi.org/10.1016/j.surfcoat.2005.12.050

[9] Amina, O., Abudukeremu, K., Raghuveer, S., *et al.* (2022) A Comprehensive Review on Green Perspectives of Electrocoagulation Integrated with Advanced Processes for Effective Pollutants Removal from Water Environment. *Environmental Research*, **215**, Article ID: 114294. https://doi.org/10.1016/j.envres.2022.114294

[10] Martina, V., Riccardis, F. and Carbone, D. (2010) A Chemometric Study of Alumina/Peek and Hydroxyapatite/PEEK Suspensions Prepared for Electrophoretic Deposition of Multifunctional Coatings. *Advances in Science and Technology*, **66**, 29-34. https://doi.org/10.4028/www.scientific.net/AST.66.29

[11] Jothi, K.J. and Palanivelu, K. (2014) Facile Fabrication of Core-Shell $Pr_6O_{11}$-ZnO Modified Silane Coatings for Anti-Corrosion Applications. *Applied Surface Science*, **288**, 60-68. https://doi.org/10.1016/j.apsusc.2013.09.112

[12] Majdi, M.R., Danaee, I., Seyyed, S. and Seyyed, A. (2017) Preparation and Anti-Corrosive Properties of Cerium Oxide Conversion Coatings on Steel X52. *Materials Research*, **20**, 445-451. https://doi.org/10.1590/1980-5373-mr-2016-0661

[13] Hee, A.C., Zhao, Y., Jamali, S.S., Bendavid, A., Martin, P.J. and Guo, H. (2019) Characterization of Tantalum and Tantalum Nitride Films on Ti6Al4V Substrate Prepared by Filtered Cathodic Vacuum Arc Deposition for Biomedical Applications. *Surface and Coating Technology*, **365**, 24-32. https://doi.org/10.1016/j.surfcoat.2018.05.007

[14] Shen, C.W. and Wen, C.J.W. (2003) Kinetics of Electroplating Process of Nano-Sized Ceramic Particle/Ni Composite. *Materials Chemistry and Physics*, **78**, 574-580. https://doi.org/10.1016/S0254-0584(01)00564-8

[15] Guglielmi, N. (1972) Kinetics of the Deposition of Inert Particles from Electrolytic Baths. *Journal of the Electrochemical Society*, **119**, 1009-1012. https://doi.org/10.1149/1.2404383

[16] Celis, J.P., Roos, J.R. and Buelens, C. (1987) A Mathematical Model for the Electrolytic Co-Deposition of Particles with a Metallic Matrix. *Electrochemical Science and Technology*, **134**, 1402-1407. https://doi.org/10.1149/1.2100680

[17] Regis, M., Bellare, A., Pascolini, T. and Bracco, P. (2017) Characterization of Thermally Annealed PEEK and CFR-PEEK Composites: Structure-Properties Relationships. *Polymer Degradation and Stability*, **136**, 121-130. https://doi.org/10.1016/j.polymdegradstab.2016.12.005

[18] Low, C.T.J., Wills, R.G.A. and Walsh, F.C. (2006) Electrodeposition of Composite Coatings Containing Nanoparticles in a Metal Deposit. *Surface and Coatings Technology*, **201**, 371-383. https://doi.org/10.1016/j.surfcoat.2005.11.123

[19] González-Castillo, E.I., Žitňan, M., Torres, Y., Shuttleworth, P.S., Galusek, D., Ellis, G. and Boccaccini, A.R. (2022) Relation between Chemical Composition, Morphology, and Microstructure of Poly(ether ether ketone)/Reduced Graphene Oxide Nanocomposite Coatings Obtained by Electrophoretic Deposition. *Journal of Material Science*, **57**, 5839-5854. https://doi.org/10.1007/s10853-022-06995-2

[20] Jeong, D.H., Gonzalez, F., Palumbo, G., Aust, K.T. and Erb, U. (2001) The Effect of Grain Size on the Wear Properties of Electrodeposited Nanocrystalline Nickel Coatings. *Scripta Materialia*, **44**, 493-499.
https://doi.org/10.1016/S1359-6462(00)00625-4

[21] Radwan, A.B., Sliem, M.H., Yusuf, N.S., Alnuaimi, N.A. and Abdullah, A.M. (2019) Enhancing the Corrosion Resistance of Reinforcing Steel Under Aggressive Operational Conditions Using Behentrimonium Chloride. *Scientific Reports*, **9**, Article No. 18115. https://doi.org/10.1038/s41598-019-54669-y

[22] Abas, W.A., Rahmati, B., Sarhan, A.D. and Basirun, W.J. (2016) Ceramic Tantalum Oxide Thin Film Coating to Enhance the Corrosion and Wear Characteristics of Ti-6Al-4V Alloy. *Journal of Alloys and Compounds*, **676**, 369-376.
https://doi.org/10.1016/j.jallcom.2016.03.188

[23] Glocker, R. and Kaupp, E. (1924) Über die Faserstruktur elektrolytischer Metallniederschläge. *Zeitschrift für Physik*, **24**, 121-139. https://doi.org/10.1007/BF01327239

[24] Cho, J.Y. and Szpunar, J.A. (2002) The Effect of Substrate Texture and Electroplating Conditions on the Texture and Surface Morphology of Copper Electrodeposits. *Materials Science Forum*, **408**-**412**, 1609-1614.
https://doi.org/10.4028/www.scientific.net/MSF.408-412.1609

[25] Lu, F., Song, B., He, P., Wang, Z. and Wang, J. (2017) Electrochemical Impedance Spectroscopy (EIS) Study on the Degradation of Acrylic Polyurethane Coatings. *RSC Advances*, **7**, 13742. https://doi.org/10.1039/C6RA26341K
https://pubs.rsc.org/en/content/articlelanding/2017/RA/C6RA26341K

[26] Takada, H., Okada, K., Koga, T. and Hirabayashi, H. (1991) Relation between Preferred Orientation and Young Primes Modulus of Electroplated Nickel. *Journal of the Japan Institute of Metals*, **55**, 12-20. (In Japan)
https://doi.org/10.2320/jinstmet1952.55.12_1368

[27] Pogrebnjak, A., Buranich, V., Ivashchenko, V., Baimoldanov, L., Rokosz, K., Steinar, R., Pawel, Z.O., Bauyrzhan, R., Vyacheslav, B. and Nazgul, E. (2022) The Effect of Substrate Treatment on the Properties of TiAlSiYN/CrN Nanocomposite Coatings. *Surfaces and Interfaces*, **30**, Article ID: 101902.
https://doi.org/10.1016/j.surfin.2022.101902

[28] Alfantazi, A.M., Brehaut, G. and Erb, U. (1997) The Effects of Substrate Material on the Microstructure of Pulse-Plated Zn-Ni Alloys. *Surface and Coatings Technology*, **89**, 239-244. https://doi.org/10.1016/S0257-8972(96)02894-0

[29] Pangarov, N.A. (1962) The Crystal Orientation of Electrodeposited Metals. *Electrochimica Acta*, **7**, 139-146. https://doi.org/10.1016/0013-4686(62)80023-1

[30] Pangarov, N.A. and Vitkova, S.D. (1966) Preferred Orientation of Electrodeposited Iron Crystallites. *Electrochimica Acta*, **11**, 1719-1731.
https://doi.org/10.1016/0013-4686(66)80085-3

[31] Evans, D.J. (1958) The Structure of Nickel Electrodeposits in Relation to Some Physical Properties. *Transactions of the Faraday Society*, **54**, 1086-1091.
https://doi.org/10.1039/tf9585401086

[32] Vadim, V., Galina, O., Elena, G., Eduard, A., *et al.* (2016) Development of Complete Color Palette Based on Spectrophotometric Measurements of Steel Oxidation Re-

sults for Enhancement of Color Laser Marking Technology. *Materials & Design*, **89**, 684-688. https://doi.org/10.1016/j.matdes.2015.10.030

[33] Sheikh, A.F., Ankush, R., Sanjay, M., Ramachandra, A.S., Subramanian, J. and Mir, I.H. (2022) Nanostructured Coatings: Review on Processing Techniques, Corrosion Behaviour and Tribological Performance. *Nanomaterials*, **12**, 1323. https://doi.org/10.3390/nano12081323

[34] Czerwinski, F. and Szpunar, J.A. (1999) Controlling the Surface Texture of Nickel for High Temperature Oxidation Inhibition. *Corrosion Science*, **41**, 729-740. https://doi.org/10.1016/S0010-938X(98)00146-2

[35] BinSabt, M.H., Abditon, M. and Galal, A. (2022) Highly Efficient Nanocomposite-Containing Coatings for the Protection of Mg Alloy against Corrosion in Chloride Containing Electrolytes. *Applied Physics A*, **128**, 151-162. https://doi.org/10.1007/s00339-021-05248-4

[36] Lingois, P., Berglund, L., Greco, A. and Maffezoli, A. (2003) Chemically Induced Residual Stresses in Dental Composites. *Journal of Materials Science*, **38**, 1321-1331. https://doi.org/10.1023/A:1022811315807

[37] Liu, X. and Zhang B. (2002) Effects of Grinding Process on Residual Stresses in Nanostructured Ceramic Coatings. *Journal of Materials Science*, **37**, 3229-3239. https://doi.org/10.1023/A:1016174731658

[38] Buchmann, M., Gadow, R. and Tabellion, J. (2000) Experimental and Numerical Residual Stress Analysis of Layer Coated Composites. *Materials Science and Engineering: A*, **288**, 154-159. https://doi.org/10.1016/S0921-5093(00)00862-5

[39] Jian, M.Z., Ke, W.X. and Vincent, J. (2001) Dependence of Stresses on Grain Orientations in Thin Polycrystalline Films on Substrates: An Explanation of the Relationship between Preferred Orientations and Stresses. *Applied Surface Science*, **180**, 1-5. https://doi.org/10.1016/S0169-4332(01)00243-4

[40] Jignesh, H., Vipin, C. and Ramesh, C. (2021) Anticorrosive Behavior Enhancement of Stainless Steel 304 through Tantalum-Based Coatings: Role of Coating Morphology. *Journal of Materials Engineering and Performance*, **30**, 1895-1905. https://doi.org/10.1007/s11665-021-05542-5

[41] Mimani, T. and Patil, K.C. (2001) Solution Combustion Synthesis of Nanoscale Oxides and Their Composites. *Materials Physics and Mechanics*, **4**, 134-137. https://mpm.spbstu.ru/article/2001.6.14/ https://doi.org/10.1016/S0894-7317(01)70064-8

[42] Ashish, K.K., Muhammad, U.B., Zulfiqar, A.K. and Pradeep, L.M. (2020) Corrosion Performance of Nanocomposite Coatings in Moist $SO_2$ Environment. *The International Journal of Advanced Manufacturing Technology*, **106**, 4769-4776. https://doi.org/10.1007/s00170-020-04949-z

[43] Seyedeh, P.M., Abdukeremu, K., Raghuveer, S., Razieh, A., Maryam, S., Jun, L., Nur, S.Z. and Farooq, S. (2022) Superior Removal of Humic Acid from Aqueous Stream Using Novel Calf Bones Charcoal Nanoadsorbent in a Reversible Process. *Chemosphere*, **301**, Article ID: 134673. https://doi.org/10.1016/j.chemosphere.2022.134673

## Nomenclature

CD: current density;

DC: direct current;

EDS: energy dispersive X-ray spectroscopy;

I: electric current;

MTM: mathematical model for the electrolytic codeposition;

SEM: scanning electron microscope;

t: time of coating;

TEM: transmission electron microscope;

XRD: X-ray diffraction;

$Ni_{wt}$: weight of coated Nickel;

$A_{coated}$: cross-sectional area of the coated layer;

$\delta$: diffusion double layer;

$\rho_{Ni}$: density of the coated Nickel.